THE JOURNAL OF BIOLOGICAL CHEMISTRY VOL. 288, NO. 45, pp. 32506–32516, November 8, 2013

Inhibition of Snail1-DNA-PKcs Protein-Protein Interface Sensitizes Cancer Cells and Inhibits Tumor Metastasis*

Received for publication, April 24, 2013, and in revised form, September 13, 2013 Published, JBC Papers in Press, October 1, 2013, DOI 10.1074/jbc.M113.479840

Ga-Young Kang[‡1], Bo-Jeong Pyun[‡1,2], Haeng Ran Seo[§3], Yeung Bae Jin[¶], Hae-June Lee[§], Yoon-Jin Lee[§], and Yun-Sil Lee[‡4]

From the [‡]College of Pharmacy, Graduate School of Pharmaceutical Sciences, Ewha Womans University, Seoul 120-750, the [§]Division of Radiation Effects, Korea Institute of Radiological and Medical Sciences, Seoul 139-706, and the [¶]Korea Atomic Energy Research Institute, Advanced Radiation Technology Institute, Jeongeup-si, Jeollabuk-do 580-185, Korea

Background: Previously, we identified the interaction between DNA-PKcs and Snail1.
Results: Inhibition of the interaction between two molecules using Snail1 peptide (7-amino acid construct) sensitized cancer cells and inhibited tumor migration.
Conclusion: Interfering with the protein-protein interaction between DNA-PKcs and Snail1 may be an effective strategy for cancer treatment.
Significance: Interfering with the interaction between DNA-PKcs and Snail1 may be a novel target for cancer treatment.

Our previous study suggested that the DNA-dependent protein kinase catalytic subunit (DNA-PKcs) interacts with Snail1, which affects genomic instability, sensitivity to DNA-damaging agents, and migration of tumor cells by reciprocal regulation between DNA-PKcs and Snail1. Here, we further investigate that a peptide containing 7-amino acid sequences (amino acids 15–21) of Snail1 (KPNYSEL, SP) inhibits the endogenous interaction between DNA-PKcs and Snail1 through primary interaction with DNA-PKcs. SP restored the inhibited DNA-PKcs repair activity and downstream pathways. On the other hand, DNA-PKcs-mediated phosphorylation of Snail1 was inhibited by SP, which resulted in decreased Snail1 stability and Snail1 functions. However, these phenomena were only shown in p53 wild-type cells, not in p53-defective cells. From these results, it is suggested that interfering with the protein interaction between DNA-PKcs and Snail1 might be an effective strategy for sensitizing cancer cells and inhibiting tumor migration, especially in both Snail1-overexpressing and DNA-PKcs-overexpressing cancer cells with functional p53.

The epithelial-mesenchymal transition, a major mechanism of cancer metastasis, is initiated by repression of the epithelial adhesion molecule, E-cadherin. This repression is mediated by several transcription factors including Snail (also known as Snail1) and Slug (also known as Snail2) (1–5). In most human cancers, metastatic tumors are resistant to radiation or chemotherapy, and emerging evidence suggests a correlation between epithelial-mesenchymal transition and resistance of cancer cells to chemo and radiotherapy (6–11).

The DNA-dependent protein kinase catalytic subunit (DNA-PKcs)[5] is a DNA-activated serine/threonine protein kinase and is abundantly expressed in almost all mammalian cells. DNA-PKcs is most commonly known as a critical component in the DNA damage repair pathway, including nonhomologous end-joining repair and homologous recombinant repair. DNA-PKcs has been shown to phosphorylate several cellular proteins, including itself, the variant histone H2AX, and p53 (12–15). Homozygous knock-out mice of DNA-PKcs catalytic subunit (DNA-PKcs$^{-/-}$) are hypersensitive to ionizing radiation (IR) and chemical treatment and have defects in DNA repair activity (16–18). From this observation, one might hypothesize that DNA repair inhibitor would sensitize the tumor cells, and in some cases, reverse the resistance phenotype, when administered in combination with drugs and/or irradiation. However, a DNA repair inhibitor generally exhibits no specific activity in killing the tumor cells, and the screening procedure should include a DNA-damaging treatment (19, 20). Moreover, a number of studies have reported a lack of correlation between cell sensitivity/resistance to IR and down/up-regulation of DNA-PKcs expression (18, 21). DNA repair is also involved in the maintenance of genome stability, and deficient activity may contribute to neoplastic transformation, as has been repeatedly documented in relation to mismatch repair and nucleotide excision repair. DNA-PKcs is found at the end of chromosomes, suggesting a role in telomere maintenance and prevention of chromosomal end-to-end fusion (22–26). Interestingly, although DNA-PKcs is highly expressed in human cells, the other nonhomologous end-joining factors are not as abundant,

* This work was supported by a grant from the Advanced Research Center for Nuclear Excellence (2011-0031696), a grant from the Mid-career Researcher Program (2011-0013364) of the National Research Foundation of Korea (NRF), and funding by the Korean government (MEST). This work was also supported by an Ewha Global Top 5 Grant 2013 from Ewha Womans University.
[1] Both authors contributed equally to this work.
[2] Present address: Korean Medicine-Based Herbal Drug Research Group, Herbal Medicine Research Division, Korea Institute of Oriental Medicine, Daejeon 305-811, Korea.
[3] Present address: Division of Cellular Differentiation, Institute Pasteur Korea, Seongnam 463-400, Korea.
[4] To whom correspondence should be addressed: College of Pharmacy, Graduate School of Pharmaceutical Sciences, Ewha Womans University, 11-1 Daehyun-Dong, Seodaemun-Gu, Seoul 120-750, Korea. Tel.: 82-2-3277-3022; Fax: 82-2-3277-2851; E-mail: yslee0425@ewha.ac.kr.
[5] The abbreviations used are: DNA-PKcs, DNA-dependent protein kinase catalytic subunits; IR, ionizing radiation; SP, Snail peptide; CP, control peptide; Gy, grays.

and the high levels of DNA-PKcs in human cells do not impart any increased ability to repair DNA damage. If the amount of expressed DNA-PKcs essentially exceeds the demand for DNA damage repair, it is not yet understood why human cells universally express such high levels of this complex. Indeed, DNA-PKcs is also reported to be involved in metabolic gene regulation in response to insulin, independently from the nonhomologous end-joining repair system (27–29).

In our previous study, we identified a novel function of DNA-PKcs as a regulator of Snail1 (30). The direct interaction between DNA-PKcs and Snail1 induced Snail1 phosphorylation at Ser-100, which stabilized the Snail1 protein and potentiated Snail1 functions, such as E-cadherin promoter repression and metastasis properties. Snail1 phosphorylation exhibited reciprocal inhibition of DNA-PKcs kinase activity, resulting in impaired DNA damage repair and induction of chromosomal or genomic instability. In this study, we further utilized a novel, 7-amino acid-containing Snail peptide (SP), which is included in the binding site for interaction with DNA-PKcs. In addition, SP can abrogate the DNA-PKcs-mediated Snail1 phosphorylation at Ser-100 that resulted in the blocking of Snail1-mediated radioresistance and metastasis. SP also restored DNA-PKcs-mediated repair activity, which was due to direct interaction with endogenous Snail1. These results suggest a novel strategy for anticancer therapy through inhibition of binding between DNA-PKcs and Snail1 in cancer cells with overexpression of both DNA-PKcs and Snail1. This approach highlights how protein-protein interfaces can be exploited to develop novel targets, which can be used to dissect signal transduction mechanisms and provide leads for novel therapeutics to target specific Snail1-DNA-PKcs protein-protein interactions in cancer cells.

EXPERIMENTAL PROCEDURES

Plasmids—DNA-PKcs deletion constructs were generated using PCR, by isolating internal regions from the full-length cDNA for DNA-PKcs, kindly given to us by Dr. Katheryn Meek (Michigan State University, East Lansing, MI). PCR fragments were inserted into the pCMV6 (31) expression vector using NotI and KpnI restriction sites; products were sequenced for verification (Cosmogenetech Co., Ltd., Seoul, Korea). Expression vectors pCR3.1-Snail1-FLAG and Snail1 mutant proteins with FLAG epitope tails, including the S100A mutant, were prepared as described previously (32, 33).

Cell Culture and Transfection—DLD-1 human colorectal adenocarcinoma cells, M059J/M059K human glioblastoma cells, and CT26 murine colon carcinoma cells were cultured in Dulbecco's minimal essential medium (DMEM; Life Technologies), supplemented with heat-inactivated 10% fetal bovine serum (FBS; Life Technologies) and antibiotics. The expression of peptides (4 μM) was introduced into cells using Lipofectamine® 2000 transfection reagent (Invitrogen).

Antibodies and Reagents—Cycloheximide, propidium iodide, and a monoclonal antibody for FLAG were purchased from Sigma. Monoclonal antibodies for DNA-PKcs, Ku86, p53, predesigned siRNAs for human DNA-PKcs, and a negative control siRNA were purchased from Santa Cruz Biotechnology (Santa Cruz, CA). Anti-Snail1 and phospho-p53 were purchased from Cell Signaling Technology (diluted 1:1000, Danvers, MA). Anti-phospho-DNA-PKcs (Ser-2056) was purchased from Abcam (diluted 1:1000, Cambridge, MA), and γ-H2AX was purchased from Millipore (diluted 1:1000, Billerica, MA). Anti-phospho-Snail1 (Ser-100) was raised in a rabbit through inoculation with a synthetic peptide, corresponding with the residues of human Snail1 (phosphorylated at Ser-100) and further purified by affinity chromatography (diluted 1:1000, Young In Frontier, Seoul, Korea). Control peptide and Snai1 peptide were purchased from AnyGen (Jangseong-gun, Korea). TGF-β1 was purchased from BD Biosciences.

Immunoblotting and Immunoprecipitation—For immunoblotting, cells were lysed with radioimmune precipitation buffer (50 mM Tris-HCl (pH 7.5), 150 mM NaCl, 1% Nonidet P-40, 0.1% SDS, and 1% sodium deoxycholate) supplemented with 1 mM Na_3VO_4, 1 mM DTT, 1 mM NaF, and protease inhibitor mixture (Roche Applied Science). The samples were boiled for 5 min, and an equal amount of protein was analyzed on SDS-PAGE.

For immunoprecipitation, cells (1×10^7) were lysed in immunoprecipitation buffer (50 mM HEPES, pH 7.6, 150 mM NaCl, 5 mM EDTA, 0.1% Nonidet P-40). After centrifugation (10 min at 15,000 $\times$ *g*) to remove particulate material, supernatants were incubated with antibodies (1:100) against DNA-PKcs, biotin, and FLAG with constant agitation at 4 °C. Immunocomplexes were precipitated with protein A-Sepharose (Sigma) and analyzed by SDS-polyacrylamide gel electrophoresis using enhanced chemiluminescence detection.

Irradiation—Cells or mice were exposed to γ-ray with a ^{137}Cs γ-ray source (Atomic Energy of Canada, Mississauga, Ontario, Canada) with a dose rate of 3.18 Gy/min.

DNA-PKcs Kinase Assay—DNA-PKcs kinase activity was analyzed, using the signaTECT DNA-PKcs assay system (Promega, Madison, WI). Nuclear extracts were isolated for DNA-PKcs kinase activity analysis. The phosphorylation reactions were carried out in the presence of [γ-^{32}P]ATP (PerkinElmer Life Sciences) for 5 min at 30 °C with 25 μg of biotinylated-p53 peptide (biotin-EPPLSQEAFADLWKK; Promega) as the substrate. The efficiency of ^{32}P labeling of the substrate was measured using a PhosphorImager.

Ubiquitination Assay—For cell-based ubiquitination assays, DLD-1 cells were transfected with HA-ubiquitin constructs. After transfection, the cells were lysed with immune precipitation assay buffer, and samples were briefly sonicated. After centrifugation, clear lysates were immunoprecipitated with anti-ubiquitin (Santa Cruz Biotechnology) antibodies. Immunocomplexes were analyzed by Western blot, using anti-ubiquitin or anti-Snail1 antibodies.

E-cadherin Promoter Assays—Cells growing at ~70% confluence in 60-mm dishes were transfected using Lipofectamine® 2000 transfection reagent (Invitrogen) according to the manufacturer's protocol. For experiments assessing activation of 1 μg of pGL3-control vector (Promega) or E-cadherin reporter gene construct by endogenous factors, 1 μg of E-cadherin reporter gene construct and 200 ng of β-galactosidase expression vector were transfected into cells. The cells were harvested 48 h after transfection using reporter lysis buffer (Promega) followed by determination of luciferase and β-galactosidase activities. All results represent the mean of three independent experiments.

Migration Assay—Cell migration was assayed using a Boyden chamber assay, as described previously (34). Cells were harvested with trypsin (0.1 mg/ml), centrifuged, counted, and resuspended in serum-free media. The cells were plated on the upper side of a collagen-treated, polycarbonate membrane, separating the two chambers of 6.5-mm Transwell culture plates (Costar, Corning, NY). After 16 h, the cells on the upper face of the membrane were scraped using a cotton swab, and the cells that migrated to the lower face of the membrane were stained with DiffQuick Wright-Giemsa solution (Baxter, Deerfield, IL).

Linear dsDNA-associated Protein Pulldown Assay—Nuclear extracts were isolated for a dsDNA pulldown assay. A biotinylated oligonucleotide (1 kb), which was generated by PCR amplification of pcDNA3 (5.4 kb) with the biotinylated forward primer 5′-GACTCTCAGTACAATCTGCTCTGA-3′ and reverse primer 5′-AGCTCTAGCATTTAGGTGACACT-3′, was immobilized on streptavidin beads (Sigma). Immobilized DNA was mixed with nuclear extracts and incubated for 3 h at 4 °C. The beads were washed with buffer D (10 mM Tris, pH 7.6, and 100 mM NaCl) and boiled for 5 min in 2× SDS sample buffer. Double-stranded DNA-associated proteins were analyzed by SDS-PAGE using enhanced chemiluminescence detection (ECL, Amersham Biosciences).

Immunofluorescence Analysis—For immunofluorescence analysis, cells were fixed with 4% paraformaldehyde, permeabilized with 0.1% Triton X-100 in PBS, and then washed three times with PBS. The cells were then incubated with anti-DNA-PKcs or anti-biotin diluted to 1:200 in PBS with 5% FBS for 1 h at room temperature in a humidified chamber. Excess antibody was removed by washing the coverslips three times with PBS. The cells were then incubated with Alexa Fluor-488 (green) and Alexa Fluor-568 (red) secondary antibodies (Invitrogen) at a 1:200 dilution in PBS with 5% FBS for 2 h. After washing three times with PBS, coverslips were mounted onto microscope slides using ProLong anti-fade mounting reagent (Molecular Probes, Eugene, OR). The slides were analyzed using a confocal laser-scanning microscope (Leica Microsystems, Wetzlar, Germany).

Cell Cycle Analysis—For cell cycle analysis, the cells were fixed in 70% ethanol at −20 °C for at least 18 h. The fixed cells were washed once with PBS-EDTA and resuspended in 1 ml of PBS. After the addition of 10 μl each of propidium iodide (5 mg/ml) and RNase (10 mg/ml), the samples were incubated for 30 min at 37 °C and analyzed using a FACScan flow cytometer (BD Biosciences).

Comet Assay—The cells were exposed to IR (5 Gy) and subjected to a comet assay to detect DNA damage and repair at the single-cell level, using a commercially available assay system (Trevigen, Gaithersburg, MD). Briefly, after treatment with IR, cells were harvested and mixed with low melting temperature agarose. After lysis, electrophoresis was performed at 1 V cm^{-1} and 15 mA for 40 min. Slides were stained with SYBR green dye for 10 min. Twenty randomly selected cells per sample were captured under a Zeiss fluorescent microscope, and digital fluorescent images were obtained using Comet software (Andor, Belfast, UK). The comet distance moment was proportional to the amount of DNA damage present in the individual nuclei and was measured by the Olive tail moment using the Comet software.

Lung Colonization Assay—All protocols involving mice were approved by the Institutional Animal Care and Use Committee of Ewha Womans University. To generate lung metastases, 2×10^6 CT26 cells were injected into the tail vein of C57BL6 mice (Central Lab. Animal Inc., Seoul, Korea). Two days later, measurement of 3 Gy of whole body irradiation was performed. Intraperitoneal injection of control peptide (CP) or SP at 3 mg/kg in PBS was performed once before IR and four times after IR. Lungs were harvested 2 weeks after cell injection, weighed, and fixed in formalin. Colony number and colony area in lung were counted.

Statistical Analyses—A Student's *t* test and an analysis of variance were used to determine significant differences between the experimental groups. Statistical analyses were performed using GraphPad Prism 5.0 (GraphPad Software, Inc.).

RESULTS

DNA-PKcs Interacts with Both Snail1 and Slug—Our previous study suggested that Snail1 interacts with DNA-PKcs (30), and Snail1 and Slug belong to the same Snail super family of zinc finger transcription factors (35–38). When DLD-1 cells overexpressed FLAG-Snail1 or FLAG-Slug, immunoprecipitated DNA-PKcs bound to both Snail1 and Slug (Fig. 1*A*). Sequence analysis of Snail1 and Slug revealed that only amino acids 15–21 of Snail1 and Slug showed sequence homology. Because these sequences have only 7 overlapping amino acids (KPNYSEL), we were able to synthesize these SPs. A CP, made up of an amino acid sequence that was not homologous to either Snail1 or Slug, was also prepared (NPEFTFQ). Biotin-labeled SP interacted with DNA-PKcs; however, biotin-labeled CP did not (Fig. 1*B*, *left*). Interaction between Snail1 and DNA-PKcs was inhibited by an increased addition of SP to Snail1-overexpressing cells (Fig. 1*B*, *middle* and *right*). Immunofluorescence data also revealed that biotin-labeled SP co-localized with DNA-PKcs in nucleus of the cells, but biotin-labeled CP did not (Fig. 1*C*). When we added Site 7, amino acids 3534–4129 of the kinase domain of DNA-PKcs, which is the binding site of DNA-PKcs for interaction with Snail1, binding of biotin-labeled SP with Site-7 occurred. This suggests that SP interacted with DNA-PKcs at the Snail binding site (Fig. 1*D*). To examine the physiological relevance, samples were treated with TGF-β, transcriptional activator of Snail1 (39–41), and binding activity was detected. Increased binding activity between DNA-PKcs and Snail1 by TGF-β was inhibited by additional SP transfection (Fig. 1*E*). The peptide sequences selected from Snail1 and Slug, hypothesized to interact with DNA-PKcs, included 7 amino acids, and treatment of this peptide inhibited endogenous binding activity between Snail1 (or Slug) and DNA-PKcs.

SP Activates DNA Repair Activity and Inhibits DNA-PKcs-mediated Snail1 Phosphorylation at Ser-100 after IR—We hypothesized that SP might interfere with direct interaction between DNA-PKcs and Snail1. To confirm this, we examined the downstream pathway of DNA-PKcs after IR. SP treatment potentiated IR-induced phosphorylation of DNA-PKcs at Ser-2056 and of p53 at Ser-15 and γ-H2AX when compared with

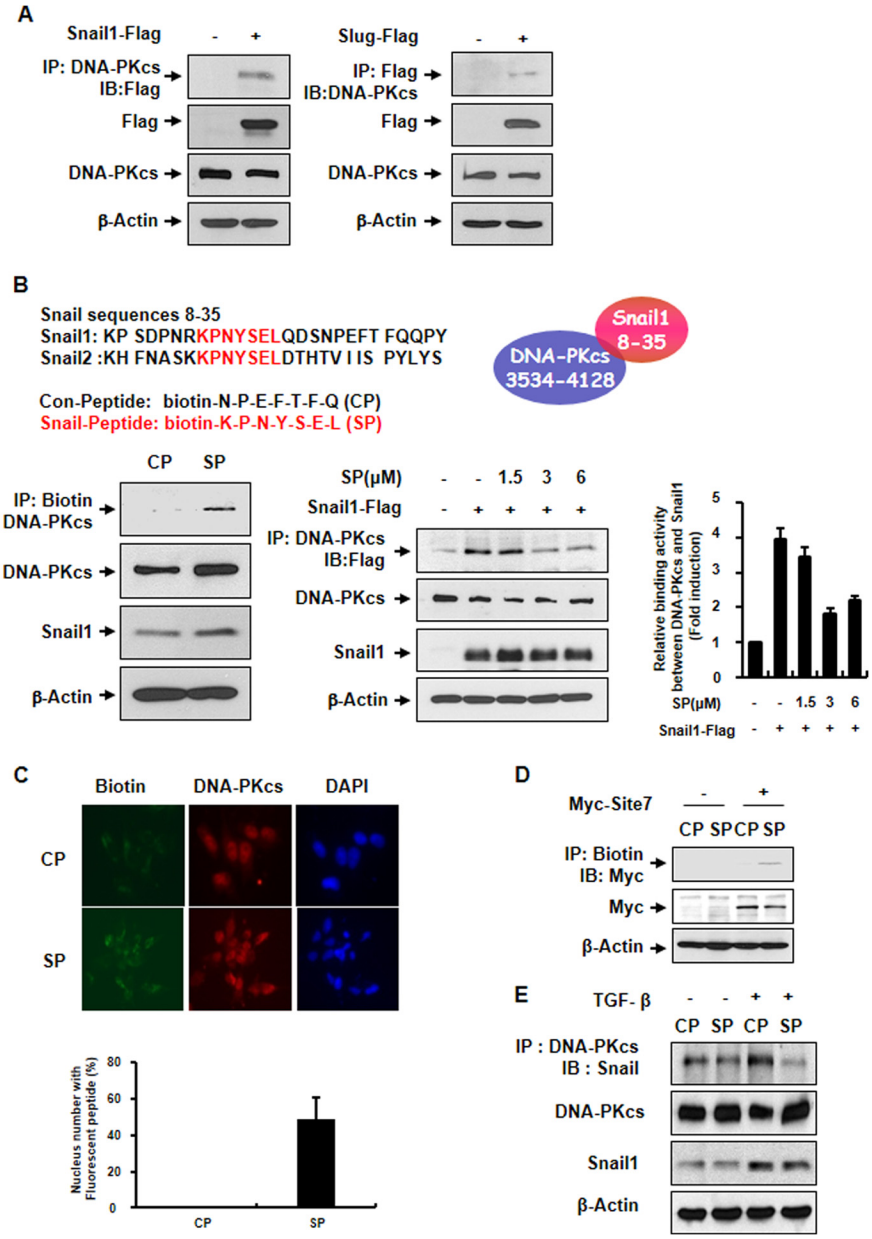

FIGURE 1. **DNA-PKcs interacts with both Snail1 and Slug.** *A*, FLAG-tagged Snail1 or FLAG-tagged Slug was transfected into DLD-1 cells. Western blotting or immunoblotting (*IB*) was conducted following immunoprecipitation (*IP*) using cell extracts. *B*, CP (4 μM) and SP (4 μM) were transfected into DLD-1 cells (*left*) or SP (0, 1.5, 3, and 6 μM) was transfected into a vector control or FLAG-tagged Snail1-overexpressing cells. After 24 h, the cells were harvested, and lysates were generated for immunoprecipitation and immunoblotting (*middle*). The relative binding activity between Snail1 and DNA-PKcs was calculated by comparing densitometric scans of the sample immunoblots after immunoprecipitation with the values of control samples set at 1 (*right*). *Error bars* indicate mean ± S.D. *C*, DLD-1 cells were transfected with biotin-labeled CP or SP (each 4 μM). The cells were immunostained for detection of peptide (*green*) and DNA-PKcs (*red*). DNA was stained with DAPI. Localization was analyzed by confocal microscopy. *Error bars* indicate mean ± S.D. *D*, c-Myc-tagged, truncated DNA-PKcs constructs (amino acids 3534–4129 of the kinase domain, Site 7) were transfected into CP- and SP-transfected cells. Western blotting or immunoblotting were conducted following immunoprecipitation using cell extracts. *E*, after transfection of CP or SP to DLD-1 cells, TGF-β (10 ng/ml) was incubated for 24 h. Western blotting and immunoprecipitation were performed.

the results of CP-treated cells. However, in the case of DNA-PKcs knockdown cells, these differences were not observed (Fig. 2*A*). IR-induced DNA-PKcs kinase activity, using p53 peptide as a substrate, was inhibited by Snail1 overexpression; however, SP treatment restored the DNA-PKcs kinase activity when compared with the CP-treated cells. Moreover, adding Site 7 of DNA-PKcs, which can interact with SP, blocked the restoring DNA-PKcs kinase activity, which was possibly due to an endogenous interaction between Snail1 and DNA-PKcs (Fig. 2*B*). We also observed recruitment of DNA-PKcs to double-stranded breaks in DNA after transfection of DNA with double-stranded (ds) oligonucleotides (double-stranded break pulldown assay). SP increased recruitment of DNA-PKcs or Ku86 to double-stranded break sites, whereas CP did not. In the case of cells in which DNA-PKcs was knocked down through treatment with Si-DNA-PKcs, no recruitments were observed (Fig. 2*C*).

To examine its physiological relevance, we examined double-stranded break repair activity. We observed that SP treatment significantly inhibited IR-mediated comet tail production and reduced IR-mediated aneuploidy (>4N) when compared with

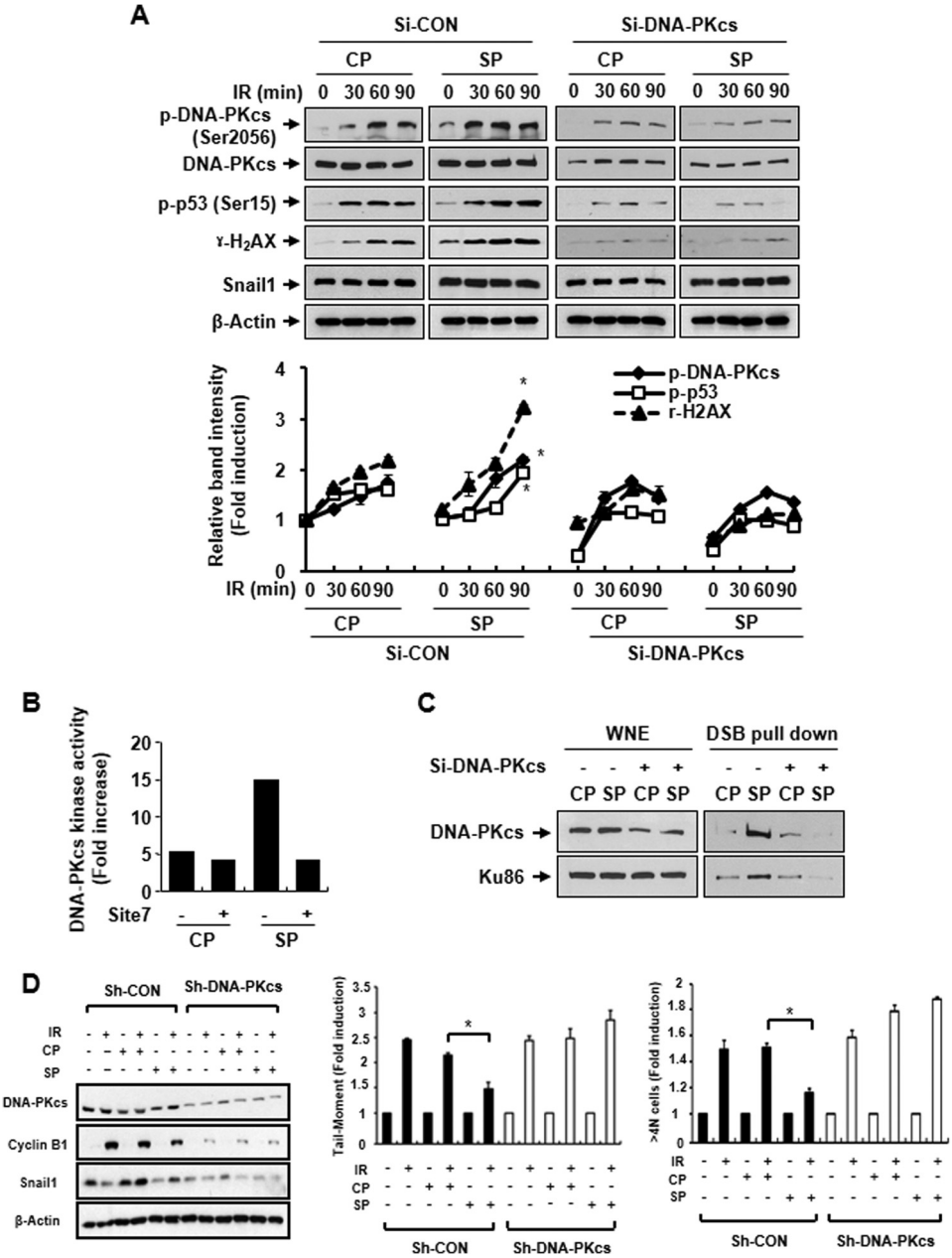

FIGURE 2. **SP activates DNA repair activity and inhibits DNA-PKcs-mediated Snail phosphorylation at Ser-100 after IR.** *A*, after transfection of CP (4 μM) or SP (4 μM) into control (*Si-CON*)- or siRNA of DNA-PKcs (*Si-DNA-PKcs*)-transfected DLD-1 cells, immunoblotting was performed at the indicated time points after exposure of the cells to 5 Gy of radiation (IR) (*upper*). The relative protein band intensity was calculated from densitometric scans of immunoblots with the control values set to 1. ($n = 3$, data are presented as mean ± S.D.) (*lower*). *, $p < 0.05$ *versus* CP-treated cells. *p* indicates phosphorylated form. *B*, CP or SP was transfected into c-Myc-tagged, truncated DNA-PKcs construct (amino acids 3534–4129 of the kinase domain, Site 7) transfected cells. An *in vitro* DNA-PKcs kinase assay was performed. The SAM membrane or 3-mm filter disc was analyzed using a PhosphorImager system, and values of Si-Con using p53 peptide as a substrate were set to 1. *C*, the protein levels of DNA-PKcs and Ku86 in the dsDNA pulldown lysates, as well as in complete whole nuclear extracts (*WNE*), were analyzed. *DSB*, double-stranded break. *D*, Sh-control (*Sh-CON*) or Sh-DNA-PKcs (*Sh-DNA-PKcs*) was stably transfected into DLD-1 cells. After 12 h of 5 Gy of IR, immunoblotting (*left*), a comet assay (*middle*), and flow cytometry analysis, after propidium iodide staining for detection of >4N cells (*right*), were performed. Experiments were performed more than three times, and data are presented as mean ± S.D. *, $p < 0.05$.

cells treated with CP; however, these phenomena were not detected in DNA-PKcs knockdown cells (Fig. 2*D*).

Phosphorylation of Snail1 at Ser-100 Is Blocked by SP, Which Results in Snail1 Protein Degradation by the Ubiquitination Pathway—Our previous data suggested that DNA-PKcs phosphorylated Snail1 at Ser-100, thereby increasing its protein stability (30). Because SP blocked interaction between DNA-PKcs and Snail1, we examined whether SP would affect DNA-PKcs-mediated Snail1 phosphorylation at Ser-100. The phosphorylation of Snail1 at Ser-100 was increased by IR in CP-treated cells; however, in the case of SP-treated cells, IR did not induce an increase in phosphorylation at Ser-100. When DNA-PKcs was knocked down, the potential of Snail1 phosphorylation at Ser-100 by IR was attenuated, and treatments of CP and SP showed no differences in the patterns of Snail1 phosphorylation (Fig. 3*A*).

Because Snail1 phosphorylation at Ser-100 increased the stability of Snail1 protein, we compared the half-life of Snail1 after

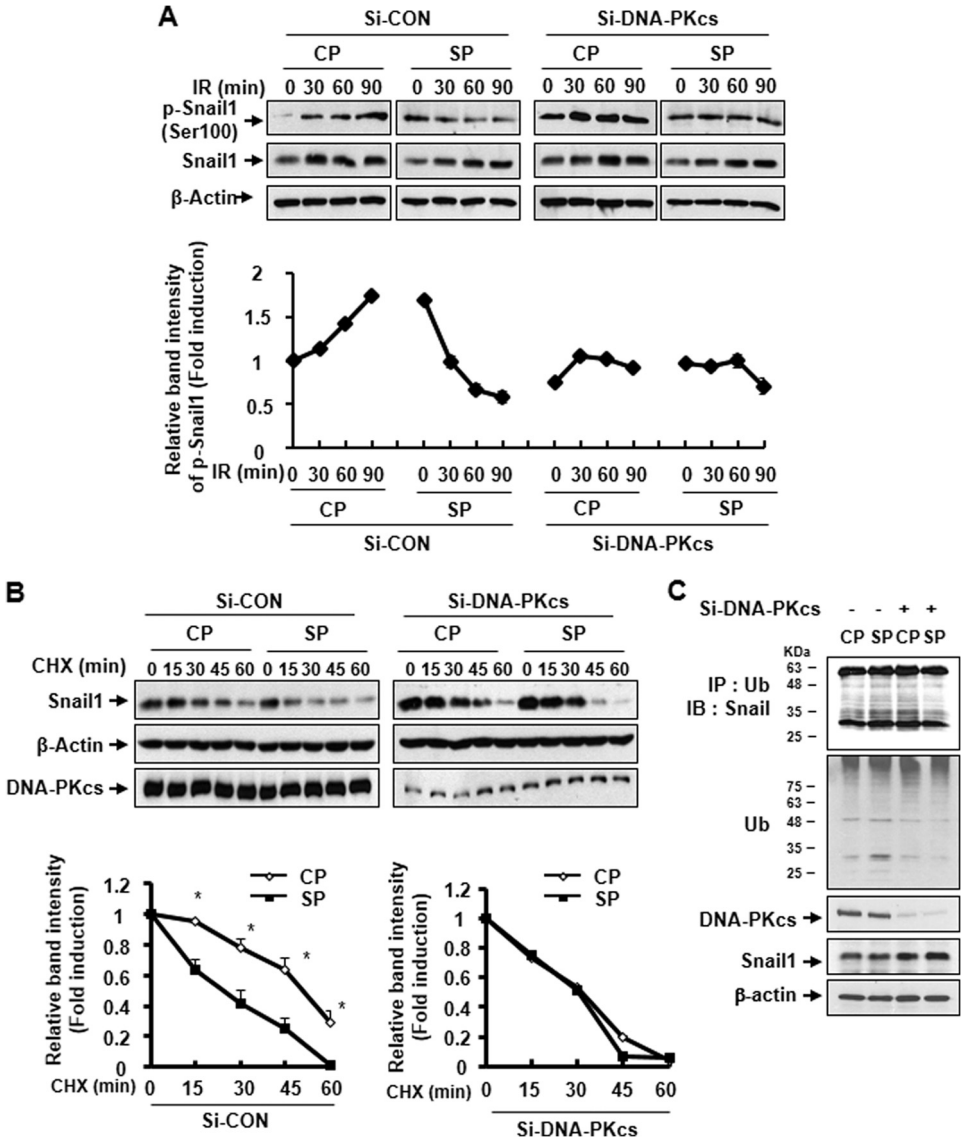

FIGURE 3. **Phosphorylation of Snail at Ser-100 is blocked by SP and results in Snail1 degradation by ubiquitination pathway.** *A*, at the indicated time points of 5 Gy of radiation (IR) after transfection of CP (4 μM) or SP (4 μM), Western blotting was performed using anti-phospho-Snail1 (*p-Snail1*) (*upper*). Relative protein band intensity was calculated by comparing densitometric scans of the sample immunoblots with the values of control samples set at 1. Result is the representative of three independent experiments (*lower*). *Si-CON*, control; *Si-DNA-PKcs*, siRNA of DNA-PKcs. *B*, protein extracts were prepared at the indicated time points following cycloheximide (*CHX*) treatment (20 μg/ml) to control (*Si-CON*)- or siRNA of DNA-PKcs (*Si-DNA-PKcs*)-transfected DLD-1 cells, also transfected with either CP or SP. Western blot analysis was performed. The relative protein band intensity was calculated from densitometric scans of immunoblots with the control values set at 1 ($n = 3$, data are presented as means $\pm$ S.D. *, $p < 0.05$ *versus* CP-treated cells). *C*, for ubiquitination assays, CP or SP was transfected into control (*Si-CON*) or siRNA of DNA-PKcs (*Si-DNA-PKcs*)-transfected DLD-1 cells. Cell lysates were immunoprecipitated (*IP*) and immunoblotted (*IB*). *Ub*, ubiquitin.

treatment with SP by using cycloheximide to block protein synthesis. SP treatment appeared to result in a shorter half-life of Snail1 when compared with CP-treated cells. However, these differences were not shown in DNA-PKcs knockdown cells (Fig. 3*B*). Indeed, ubiquitination patterns also indicated that ubiquitinated Snail1 was increased by SP treatment when compared with the CP-treated cells (Fig. 3*C*).

SP Increases E-cadherin Promoter Activity and Inhibits Tumor Migration—To elucidate whether the inhibition of Snail1 phosphorylation at Ser-100 by SP affected Snail1 function, we examined E-cadherin promoter activity, which is reported to be inhibited by Snail1. E-cadherin promoter activity was higher in SP-treated cells than in CP-treated cells. The knockdown of DNA-PKcs increased E-cadherin promoter activity; however, SP treatment did not increase E-cadherin promoter activity. These phenomena were also observed when wild-type (M059K) and DNA-PKcs-deleted (M059J) cells were used (Fig. 4*A*). We also examined the protein expression of E-cadherin, and similar effects were observed (Fig. 4*B*). Also, migration activity was inhibited by SP treatment; however, migration activity of DNA-PKcs knockdown cells was not affected by SP treatment (Fig. 4*C*). As Snail1 function is necessary for tumor metastases and expansion, we examined whether SP affected the Snail1-mediated growth of lung metastasis in animal models. Stable transfection of murine CT26 colon carcinoma cells with Snail1 WT or Snail1 S100A (phospho-defective mutant) was performed and controlled. Transfected cells were injected into mice by tail vein to generate lung

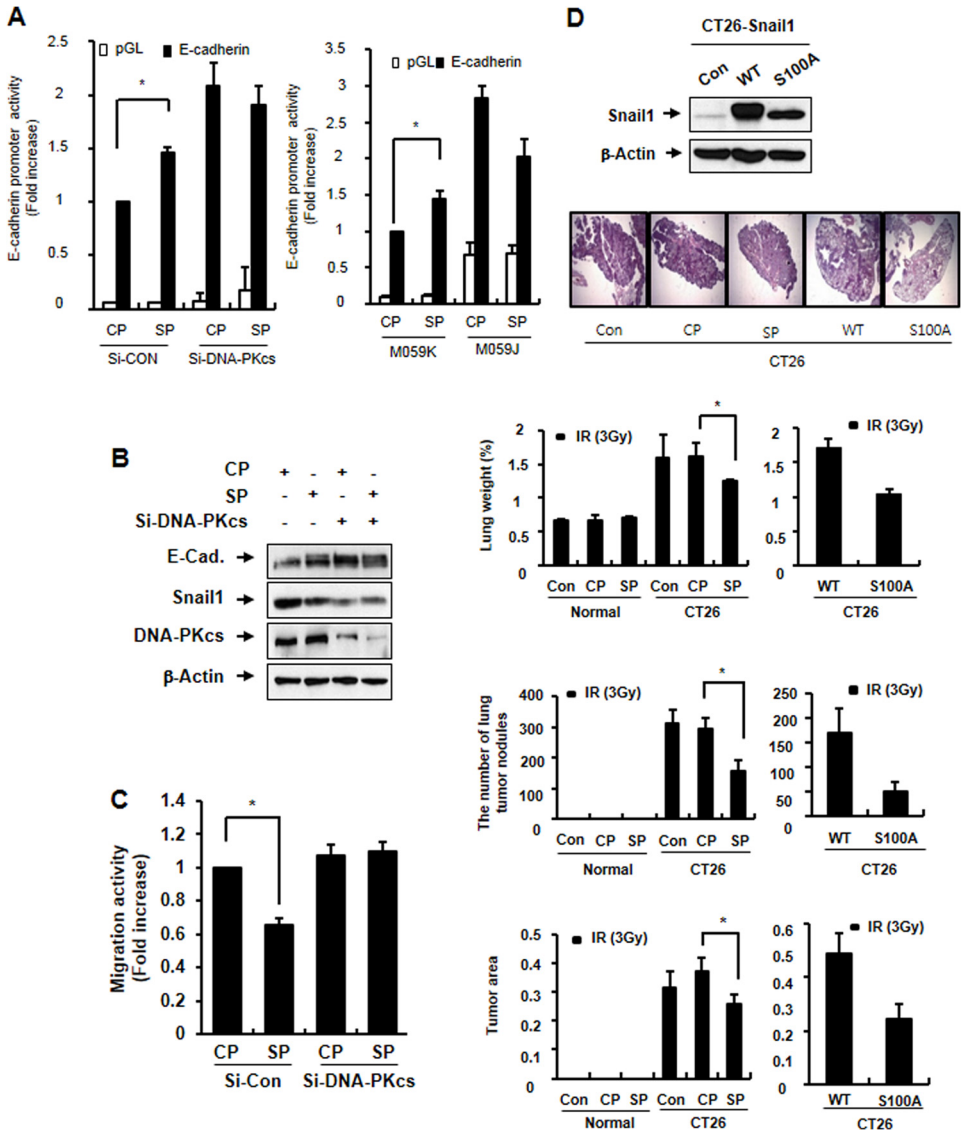

FIGURE 4. **SP increases E-cadherin promoter activity and inhibits tumor migration.** *A*, control (*Si-CON*) or siRNA of DNA-PKcs (*Si-DNA-PKcs*)-treated DLD-1 cells (*left*) or M059K and MO59J cells (*right*) with transfection of CP (4 μM) or SP (4 μM) were transiently transfected with E-cadherin promoter construct fused to a luciferase reporter gene. A luciferase assay was then performed. The E-cadherin promoter activity of CP-treated cells was set at 1. Data are presented as mean ± S.D. *, $p < 0.05$. *B*, after transfection of CP or SP to control (*Si-Con*) or siRNA of DNA-PKcs (*Si-DNA-PKcs*)-transfected DLD-1 cells, Western blotting was performed. *E-Cad.*, E-cadherin. *C*, after transfection of CP or SP to control (*Si-Con*) or siRNA of DNA-PKcs (*Si-DNA-PKcs*)-transfected DLD-1 cells, cellular invasiveness was compared. Data are presented as mean ± S.D. *, $p < 0.05$. *D*, after stable transfection of Snail1 WT or mutant Snail1 S100A plasmids to CT26 colon carcinoma cells, Western blot analysis was performed (*upper*). CT26 cells were intravenously injected through tail vein of the mice, and 3 Gy of radiation (IR) was administered. Intraperitoneal injection of CP or SP at 3 mg/kg in PBS was performed once before IR and four times after IR. The metastasis of CT26 cells was assessed by lung histology, lung weight, the number of lung metastatic nodules, and lung tumor area present 14 days after cell injection. Quantitative analysis of the number of lung weights (*upper*), metastatic nodules (*middle*), and tumor area (*lower*) (*Normal*, no tumor cell injection; *Con*, CT26 cell injection; *WT*, Snail1 WT; *S100A*, Snail1 S100A) was performed. Data are presented as mean ± S.D. of five mice from each group. *, $p < 0.05$.

colonies. When compared with irradiated mice after injection with control CT26 cells (3 Gy of IR alone), irradiated mice after injection with Snail1 WT overexpressed cells did not show any significant differences in lung colonies, as observed in lung weights, lung tumor nodule counts, and lung tumor area in lung tissues. Interestingly, SP treatment in combination with IR significantly inhibited lung colonies; these data were similar to those of S100A-transfected cells. However, in the case of CP treatment, no inhibition was observed (Fig. 4*D*). In summary, SP inhibited tumor metastasis by inhibition of Snail1 function.

SP Sensitizes IR-mediated Cell Death—Because SP induced restoration of DNA-PKcs kinase activity and radiation sensitivity by blocking the interaction between Snail1 and DNA-PKcs, we decided to examine cell death after IR, with and without SP. Treatment of IR with SP potentiated an increase in cell death; however, in the DNA-PKcs knockdown cells, SP did not cause this effect, indicating that SP effects were dependent upon DNA-PKcs (Fig. 5*A*). Expression of apoptosis-related molecules, such as cleaved PARP-1 and cleaved caspase 3, also suggests a synergistic effect of SP and IR (Fig. 5*B*). A clonogenic survival assay also indicated that SP potentiated IR effects (Fig. 5*C*). However, these phenomena were not observed in DNA-PKcs knockdown cells. From these results, we conclude that SP can sensitize cancer cells in combination with IR.

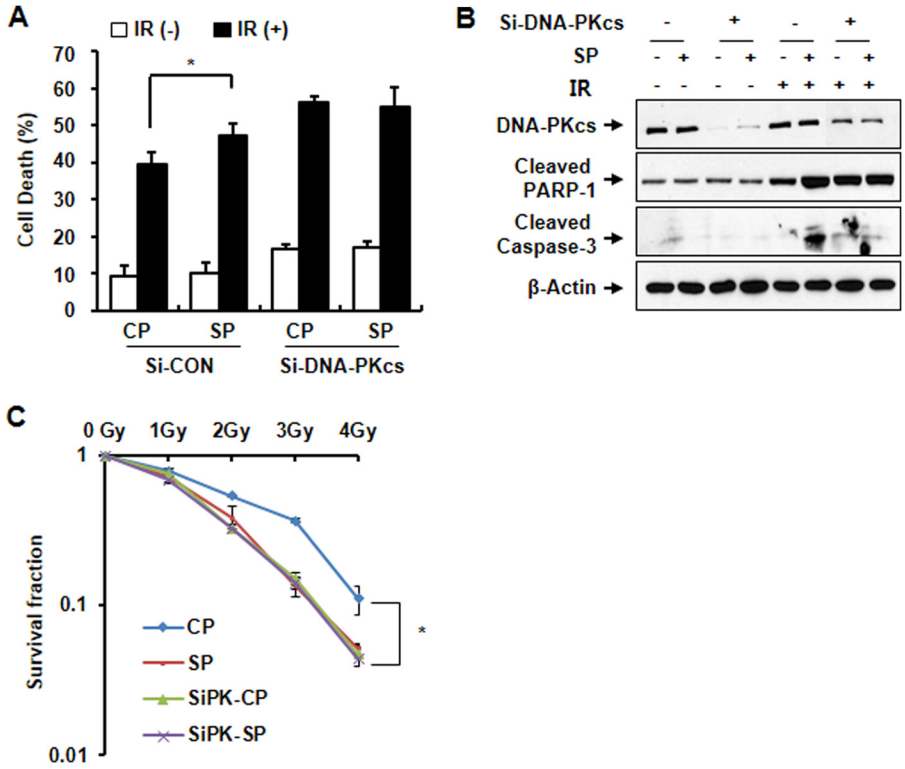

FIGURE 5. **SP sensitizes IR-mediated cell death.** *A*, after 48 h of 5 Gy of radiation (IR) was applied to DLD-1 cells transfected with CP (4 μM) or SP (4 μM), cell death was analyzed by FACS. Data are presented as mean ± S.D. *, $p < 0.05$. *Si-CON*, control; *Si-DNA-PKcs*, siRNA of DNA-PKcs. *B*, Western blot analysis was performed using anti-cleaved-caspase 3 and poly(ADP-ribose) polymerase-1 (*PARP-1*) antibodies. *C*, CP or SP were transfected into DLD-1 cells with or without siRNA of DNA-PKcs (*SiPK-CP* and *SiPK-SP*). A colony-forming assay was then conducted after the cells were treated with various doses of radiation. Data are presented as mean ± S.D. *, $p < 0.05$.

Effects of SP Are p53-dependent—Because SP treatment restored DNA-PKcs kinase and repair activity, and p53 is one of the DNA-PKcs substrates, we decided to examine whether the effects of SP were affected by p53 status. SP potentiated phosphorylation of DNA-PKcs and decreased protein stability of Snail1 in both $p53^{+/+}$ and $p53^{-/-}$ cells. Phosphorylation of p53 and γ-H2AX was also potentiated in $p53^{+/+}$ cells. However, in the case of $p53^{-/-}$ cells, no increase of phosphorylation of γ-H2AX was observed (Fig. 6*A*). A colony-forming assay, cell death detection by FACS, and caspase cleavage data also suggest that the SP sensitization of IR-mediated cell death is p53-dependent (Fig. 6, *B–D*).

DISCUSSION

The Snail1 and Slug proteins play an essential role in cancer-associated epithelial-mesenchymal transition (1–5). Although many functions of the Snail family and epithelial-mesenchymal transition are well recognized, there are still unknown mechanisms of Snail. In this study, we identified that the 7-amino acid (KPNYSEL, SP) peptide sequence, contained by both Snail1 and Slug, can interact with DNA-PKcs (Fig. 7). Treatment with SP blocked the endogenous binding activity between Snail1 and DNA-PKcs, resulting in abolishment of DNA-PKcs-mediated Snail1 phosphorylation at Ser-100 and Snail protein stability. Additionally, SP treatment provided effective sensitization of cancer cells and inhibited tumor metastasis in both Snail-overexpressing and DNA-PKcs-overexpressing cancer cells.

In our previous study, we identified a novel function of DNA-PKcs as a regulator of Snail1 (30). The direct interaction between DNA-PKcs and Snail1 induced Snail1 phosphorylation at Ser-100, which stabilized the Snail1 protein and potentiated Snail1 functions, such as E-cadherin promoter repression and metastasis properties. Snail1 phosphorylation exhibited reciprocal inhibition of DNA-PKcs kinase activity, resulting in impairment of DNA damage repair and induction of chromosomal and genomic instability.

In this study, we aimed to determine whether disruption of the protein-protein interaction between DNA-PKcs and Snail1 would give rise to similar and/or novel biological insights on the sensitization of cancer cells and inhibition of tumor metastasis. Because DNA-PKcs kinase activity is very important to DNA damage control, kinase inhibition by Snail1 phosphorylation, which was induced by TGFβ treatment, or IR may lead to more serious genomic instability of the cancer cells.

Because DNA-PKcs interacted with both Snail1 and Slug, we searched sequence homology between two proteins and found that only 7 amino acids (SP) showed sequence homology. Not only did SP interact with DNA-PKcs, it inhibited the endogenous interaction between DNA-PKcs and Snail1. SP attenuated DNA-PKcs-mediated phosphorylation of Snail1 at Ser-100, which resulted in decreased protein stability of Snail1.

In terms of physiological relevance, defective DNA damage repair and aneuploidy production can result from defective DNA-PKcs kinase activity through the interaction with Snail1. In addition, tumor migration is increased by DNA-PKcs-induced phosphorylation of Snail1 at Ser-100; however, SP treatment restored DNA-PKcs kinase activity and blocked Snail1

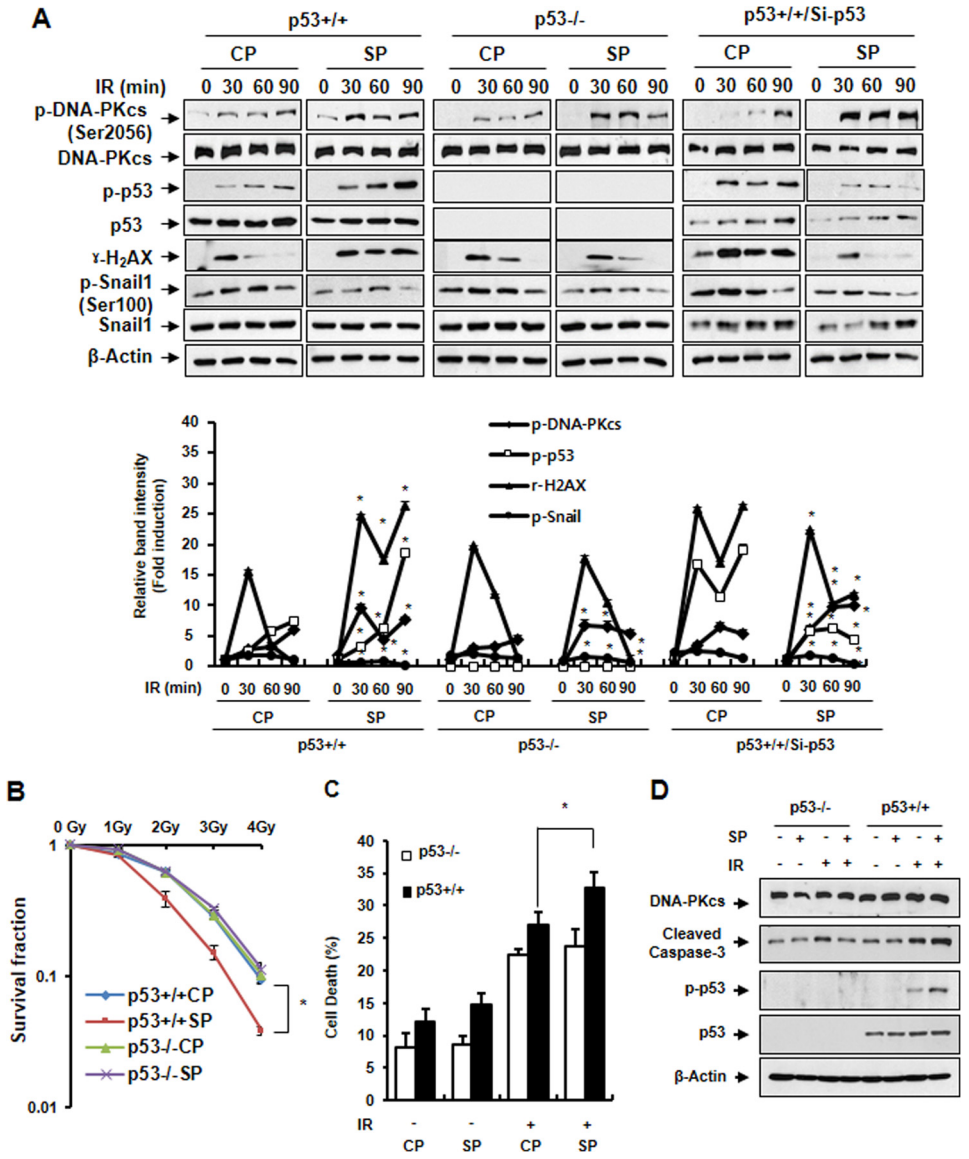

FIGURE 6. **SP shows sensitization of cancer cells in p53-dependent manner.** *A*, $p53^{+/+}$ and $p53^{-/-}$ HCT116 cells or siRNA p53 (*Si-p53*)-transfected $p53^{+/+}$ HCT cells were transiently transfected with CP (4 μM) or SP (4 μM) at the indicated time points after exposure of the cells to 5 Gy of radiation (IR). Cell lysates were obtained, and immunoblotting was performed (*upper*).*p* indicates phosphorylated form. The relative protein band intensity was calculated from densitometric scans of immunoblots with the control values set at 1. ($n = 3$, date are presented as mean ± S.D., *, $p < 0.05$ *versus* corresponding CP-treated cells.) *B*, a colony-forming assay was then conducted after the cells were treated with various doses of IR. *C*, after 48 h of 5 Gy of IR, cell death was analyzed by FACS. Data in *A–C* are presented as mean ± S.D., *, $p < 0.05$. *D*, Western blot analysis was performed.

phosphorylation. SP treatment actually sensitized cancer cells, and in combination with IR, inhibited tumor migration, or metastasis, in both *in vitro* and *in vivo* systems.

One of the targets of DNA-PKcs is p53; function of this protein is essential in DNA repair and cancer cell sensitization (42). Indeed, SP effects were only observed in p53-functional cells, not in p53-defective cells, suggesting that intact p53 function is necessary for SP-mediated inhibition of migration and sensitization of tumor cells. Of course, our finding has limitations because SP treatment alone only exhibited minor effects on the sensitization of cancer cells and inhibition of tumor metastasis. These results suggest that DNA-PKcs may be involved in only a small portion of Snail functions, especially after a DNA-damaging incident such as IR. Another limitation of our findings is that cancer cells showed p53 deletion or mutation; however, SP showed sensitization of cancer cells and inhibition of tumor metastasis only with wild-type p53. Nonetheless, because Snail1 has a critical role in cancer metastasis (1–5) and because DNA-PKcs, which we do not know much about in cancer, is an abundant protein in cancer tissue (28), inhibition of these two proteins might be an effective strategy for cancer treatment, focusing on our identification of a peptide motif as a key binding site for DNA-PKcs involved in protein-protein interactions with Snail1. This peptide found in Snail1, which competes with endogenous Snail1 for interaction with DNA-PKcs, can induce sensitization of cancer cells and inhibition of tumor metastasis. Therefore, interfering with the protein-protein interaction between DNA-PKcs and Snail1 may be an effective strategy for sensitizing cancer cells to treatment and inhibiting tumor metastasis. This concept is relatively important to address due

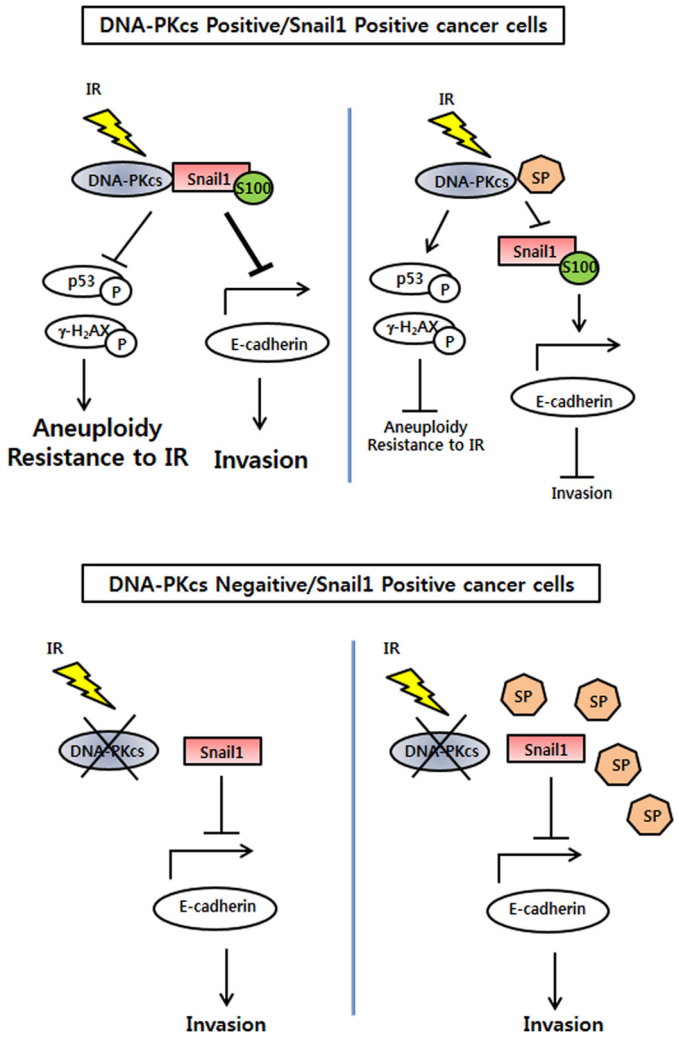

FIGURE 7. **A model illustrating that the inhibition of Snail1-DNA-PKcs protein-protein interface decreases aneuploidy, sensitizes cells to IR, and inhibits tumor metastasis.** The peptide sequences with 7 amino acids (KPNYSEL, SP), contained in both Snail1 and Slug, can interact with DNA-PKcs. Treatment with SP blocks the endogenous binding activity between Snail1 and DNA-PKcs, which results in abolishment of DNA-PKcs-mediated Snail1 phosphorylation at Ser-100 and Snail protein stability, and finally provides effective sensitization of cancer cells and inhibition of tumor metastasis in both Snail-overexpressing and DNA-PKcs-overexpressing cancer cells with functional p53. *Circled P* indicates phosphorylation.

to a growing interest in pharmaceutical development to target protein-protein interactions as a therapeutic strategy against diseases such as cancer (43).

REFERENCES

1. Barrallo-Gimeno, A., and Nieto, M. A. (2005) The Snail genes as inducers of cell movement and survival: implications in development and cancer. *Development* **132,** 3151–3161
2. Huber, M. A., Kraut, N., and Beug, H. (2005) Molecular requirements for epithelial-mesenchymal transition during tumor progression. *Curr. Opin. Cell Biol.* **17,** 548–558
3. Peinado, H., Olmeda, D., and Cano, A. (2007) Snail, Zeb and bHLH factors in tumour progression: an alliance against the epithelial phenotype? *Nat. Rev. Cancer* **7,** 415–428
4. Moreno-Bueno, G., Peinado, H., Molina, P., Olmeda, D., Cubillo, E., Santos, V., Palacios, J., Portillo, F., and Cano, A. (2009) The morphological and molecular features of the epithelial-to-mesenchymal transition. *Nat. Protoc.* **4,** 1591–1613
5. Thiery, J. P., Acloque, H., Huang, R. Y., and Nieto, M. A. (2009) Epithelial-mesenchymal transitions in development and disease. *Cell* **139,** 871–890
6. Yang, A. D., Fan, F., Camp, E. R., van Buren, G., Liu, W., Somcio, R., Gray, M. J., Cheng, H., Hoff, P. M., and Ellis, L. M. (2006) Chronic oxaliplatin resistance induces epithelial-to-mesenchymal transition in colorectal cancer cell lines. *Clin. Cancer Res.* **12,** 4147–4153
7. Kajiyama, H., Shibata, K., Terauchi, M., Yamashita, M., Ino, K., Nawa, A., and Kikkawa, F. (2007) Chemoresistance to paclitaxel induces epithelial-mesenchymal transition and enhances metastatic potential for epithelial ovarian carcinoma cells. *Int. J. Oncol.* **31,** 277–283
8. Cheng, G. Z., Chan, J., Wang, Q., Zhang, W., Sun, C. D., and Wang, L. H. (2007) Twist transcriptionally up-regulates AKT2 in breast cancer cells leading to increased migration, invasion, and resistance to paclitaxel. *Cancer Res.* **67,** 1979–1987
9. Li, Q. Q., Xu, J. D., Wang, W. J., Cao, X. X., Chen, Q., Tang, F., Chen, Z. Q., Liu, X. P., and Xu, Z. D. (2009) Twist1-mediated adriamycin-induced epithelial-mesenchymal transition relates to multidrug resistance and invasive potential in breast cancer cells. *Clin. Cancer Res.* **15,** 2657–2665
10. Kajita, M., McClinic, K. N., and Wade, P. A. (2004) Aberrant expression of the transcription factors Snail and Slug alters the response to genotoxic stress. *Mol. Cell. Biol.* **24,** 7559–7566
11. Kurrey, N. K., Jalgaonkar, S. P., Joglekar, A. V., Ghanate, A. D., Chaskar, P. D., Doiphode, R. Y., and Bapat, S. A. (2009) Snail and Slug mediate radioresistance and chemoresistance by antagonizing p53-mediated apoptosis and acquiring a stem-like phenotype in ovarian cancer cells. *Stem Cells* **27,** 2059–2068
12. Mukherjee, B., Kessinger, C., Kobayashi, J., Chen, B. P., Chen, D. J., Chatterjee, A., and Burma, S. (2006) DNA-PK phosphorylates histone H2AX during apoptotic DNA fragmentation in mammalian cells. *DNA Repair* **5,** 575–590
13. Solier, S., Sordet, O., Kohn, K. W., and Pommier, Y. (2009) Death receptor-induced activation of the Chk2- and histone H2AX-associated DNA damage response pathways. *Mol. Cell. Biol.* **29,** 68–82
14. Shieh, S. Y., Ikeda, M., Taya, Y., and Prives, C. (1997) DNA damage-induced phosphorylation of p53 alleviates inhibition by MDM2. *Cell* **91,** 325–334
15. Reitsema, T., Klokov, D., Banáth, J. P., and Olive, P. L. (2005) DNA-PK is responsible for enhanced phosphorylation of histone H2AX under hypertonic conditions. *DNA Repair* **4,** 1172–1181
16. Kirchgessner, C. U., Patil, C. K., Evans, J. W., Cuomo, C. A., Fried, L. M., Carter, T., Oettinger, M. A., and Brown, J. M. (1995) DNA-dependent kinase (p350) as a candidate gene for the murine SCID defect. *Science* **267,** 1178–1183
17. García-Barros, M., Thin, T. H., Maj, J., Cordon-Cardo, C., Haimovitz-Friedman, A., Fuks, Z., and Kolesnick, R. (2010) Impact of stromal sensitivity on radiation response of tumors implanted in SCID hosts revisited. *Cancer Res.* **70,** 8179–8186
18. Zhang, S., Yajima, H., Huynh, H., Zheng, J., Callen, E., Chen, H. T., Wong, N., Bunting, S., Lin, Y. F., Li, M., Lee, K. J., Story, M., Gapud, E., Sleckman, B. P., Nussenzweig, A., Zhang, C. C., Chen, D. J., and Chen, B. P. (2011) Congenital bone marrow failure in DNA-PKcs mutant mice associated with deficiencies in DNA repair. *J. Cell Biol.* **193,** 295–305
19. Lee, K. B., Parker, R. J., Bohr, V., Cornelison, T., and Reed, E. (1993) Cisplatin sensitivity/resistance in UV repair-deficient Chinese hamster ovary cells of complementation groups 1 and 3. *Carcinogenesis* **14,** 2177–2180
20. Youn, C. K., Kim, M. H., Cho, H. J., Kim, H. B., Chang, I. Y., Chung, M. H., and You, H. J. (2004) Oncogenic H-Ras up-regulates expression of ERCC1 to protect cells from platinum-based anticancer agents. *Cancer Res.* **64,** 4849–4857
21. Allalunis-Turner, M. J., Lintott, L. G., Barron, G. M., Day, R. S., 3rd, and Lees-Miller, S. P. (1995) Lack of correlation between DNA-dependent protein kinase activity and tumor cell radiosensitivity. *Cancer Res.* **55,** 5200–5202
22. Gilley, D., Tanaka, H., Hande, M. P., Kurimasa, A., Li, G. C., Oshimura, M., and Chen, D. J. (2001) DNA-PKcs is critical for telomere capping. *Proc. Natl. Acad. Sci. U.S.A.* **98,** 15084–15088
23. d'Adda di Fagagna, F., Hande, M. P., Tong, W. M., Roth, D., Lansdorp, P. M., Wang, Z. Q., and Jackson, S. P. (2001) Effects of DNA nonhomologous end-joining factors on telomere length and chromosomal stability in

mammalian cells. *Curr. Biol.* **11,** 1192–1196
24. Bailey, S. M., Meyne, J., Chen, D. J., Kurimasa, A., Li, G. C., Lehnert, B. E., and Goodwin, E. H. (1999) DNA double-strand break repair proteins are required to cap the ends of mammalian chromosomes. *Proc. Natl. Acad. Sci. U.S.A.* **96,** 14899–14904
25. Espejel, S., Franco, S., Sgura, A., Gae, D., Bailey, S. M., Taccioli, G. E., and Blasco, M. A. (2002) Functional interaction between DNA-PKcs and telomerase in telomere length maintenance. *EMBO J.* **21,** 6275–6287
26. Goytisolo, F. A., Samper, E., Edmonson, S., Taccioli, G. E., and Blasco, M. A. (2001) The absence of the DNA-dependent protein kinase catalytic subunit in mice results in anaphase bridges and in increased telomeric fusions with normal telomere length and G-strand overhang. *Mol. Cell. Biol.* **21,** 3642–3651
27. Wong, R. H., Chang, I., Hudak, C. S., Hyun, S., Kwan, H. Y., and Sul, H. S. (2009) A role of DNA-PK for the metabolic gene regulation in response to insulin. *Cell* **136,** 1056–1072
28. Kong, X., Shen, Y., Jiang, N., Fei, X., and Mi, J. (2011) Emerging roles of DNA-PK besides DNA repair. *Cell Signal* **23,** 1273–1280
29. Wong, R. H., and Sul, H. S. (2009) DNA-PK: relaying the insulin signal to USF in lipogenesis. *Cell cycle* **8,** 1977–1978
30. Pyun, B. J., Seo, H. R., Lee, H. J., Jin, Y. B., Kim, E. J., Kim, N. H., Kim, H. S., Nam, H. W., Yook, J. I., and Lee, Y. S. (2013) Mutual regulation between DNA-PKcs and snail1 leads to increased genomic instability and aggressive tumor characteristics. *Cell Death Dis.* **4,** e517
31. Andersson, S., Davis, D. L., Dahlbäck, H., Jörnvall, H., and Russell, D. W. (1989) Cloning, structure, and expression of the mitochondrial cytochrome P-450 sterol 26-hydroxylase, a bile acid biosynthetic enzyme. *J. Biol. Chem.* **264,** 8222–8229
32. Yook, J. I., Li, X. Y., Ota, I., Hu, C., Kim, H. S., Kim, N. H., Cha, S. Y., Ryu, J. K., Choi, Y. J., Kim, J., Fearon, E. R., and Weiss, S. J. (2006) A Wnt-Axin2-GSK3β cascade regulates Snail1 activity in breast cancer cells. *Nat. Cell Biol.* **8,** 1398–1406
33. Zhang, M. Z., Xu, J., Yao, B., Yin, H., Cai, Q., Shrubsole, M. J., Chen, X., Kon, V., Zheng, W., Pozzi, A., and Harris, R. C. (2009) Inhibition of 11β-hydroxysteroid dehydrogenase type II selectively blocks the tumor COX-2 pathway and suppresses colon carcinogenesis in mice and humans. *J. Clin. Invest.* **119,** 876–885
34. Christie, D. R., Shaikh, F. M., Lucas, J. A., 4th, Lucas, J. A., 3rd, and Bellis, S. L. (2008) ST6Gal-I expression in ovarian cancer cells promotes an invasive phenotype by altering integrin glycosylation and function. *J. Ovarian Res.* **1,** 3
35. Chiang, C., and Ayyanathan, K. (2013) Snail/Gfi-1 (SNAG) family zinc finger proteins in transcription regulation, chromatin dynamics, cell signaling, development, and disease. *Cytokine Growth Factor Rev.* **24,** 123–131
36. Nieto, M. A. (2002) The Snail superfamily of zinc-finger transcription factors. *Nat. Rev. Mol. Cell Biol.* **3,** 155–166
37. Collins, T., Stone, J. R., and Williams, A. J. (2001) All in the family: the BTB/POZ, KRAB, and SCAN domains. *Mol. Cell. Biol.* **21,** 3609–3615
38. Carver, E. A., Jiang, R., Lan, Y., Oram, K. F., and Gridley, T. (2001) The mouse Snail gene encodes a key regulator of the epithelial-mesenchymal transition. *Mol. Cell. Biol.* **21,** 8184–8188
39. Vincent, T., Neve, E. P., Johnson, J. R., Kukalev, A., Rojo, F., Albanell, J., Pietras, K., Virtanen, I., Philipson, L., Leopold, P. L., Crystal, R. G., de Herreros, A. G., Moustakas, A., Pettersson, R. F., and Fuxe, J. (2009) A SNAIL1-SMAD3/4 transcriptional repressor complex promotes TGF-β mediated epithelial-mesenchymal transition. *Nat. Cell Biol.* **11,** 943–950
40. Ding, X., Park, S. I., McCauley, L. K., and Wang, C. Y. (2013) Signaling between transforming growth factor β (TGF-β) and transcription factor SNAI2 represses expression of microRNA miR-203 to promote epithelial-mesenchymal transition and tumor metastasis. *J. Biol. Chem.* **288,** 10241–10253
41. Dhasarathy, A., Phadke, D., Mav, D., Shah, R. R., and Wade, P. A. (2011) The transcription factors Snail and Slug activate the transforming growth factor-β signaling pathway in breast cancer. *PLoS One* **6,** e26514
42. Wang, S., Guo, M., Ouyang, H., Li, X., Cordon-Cardo, C., Kurimasa, A., Chen, D. J., Fuks, Z., Ling, C. C., and Li, G. C. (2000) The catalytic subunit of DNA-dependent protein kinase selectively regulates p53-dependent apoptosis but not cell-cycle arrest. *Proc. Natl. Acad. Sci. U.S.A.* **97,** 1584–1588
43. Surade, S., and Blundell, T. L. (2012) Structural biology and drug discovery of difficult targets: the limits of ligandability. *Chem. Biol.* **19,** 42–50

Inhibition of Snail1-DNA-PKcs Protein-Protein Interface Sensitizes Cancer Cells and Inhibits Tumor Metastasis

Ga-Young Kang, Bo-Jeong Pyun, Haeng Ran Seo, Yeung Bae Jin, Hae-June Lee, Yoon-Jin Lee and Yun-Sil Lee

J. Biol. Chem. 2013, 288:32506-32516.
doi: 10.1074/jbc.M113.479840 originally published online October 1, 2013
